Journal of the Brazilian Society of Mechanical Sciences and Engineering (2020) 42:355
https://doi.org/10.1007/s40430-020-02435-x

TECHNICAL PAPER

Experimental characterization and performance of dynamic vibration absorber with tunable piecewise-linear stiffness

Muhammad Harith Mustaffer[1] · Roszaidi Ramlan[1] · Mohd Nazim Abdul Rahman[1] · Azma Putra[1]

Received: 30 October 2019 / Accepted: 25 May 2020

Abstract
Dynamic vibration absorber (DVA) is one of the ways to control the level of vibration. Among many mechanisms and control strategies of the DVA, passively tuned DVA emerges as one of the most effective absorbers due to its simple mechanism. However, the performance of the passive tuned DVA suffers from narrow suppression bandwidth. This paper introduces a nonlinear dynamic vibration absorber (NDVA) with an adjustable piecewise-linear stiffness mechanism which has a characteristic almost similar to hardening stiffness to broaden the vibration suppression bandwidth. The mechanism is made of a cantilever beam constrained by two vertically and horizontally adjustable limit blocks on either side of the beam's equilibrium position. The static and dynamic properties of the proposed NDVA were first investigated for different positions of the limit blocks. Then the performance of the NDVA was compared with the linear DVA in terms of the vibration suppression bandwidth, separation of resonance frequencies and the ability to cope with mistuning. Overall, the NDVA seems to outperform the linear DVA, and it is more forgiving in the case of mistuning.

Keywords Nonlinear vibration absorber · Hardening stiffness · Piecewise-linear stiffness

1 Introduction

Nowadays, throughout the advancement in mechanical systems and engineering structures, the demand for the vibration mitigation method has significantly increased. Until early this century, the vibration problem might not be the most significant issue due to most machines and structures usually had huge mass and damping, because of the heavy material used in their manufacturing. Since these highly damped machines or structures excitation sources were often small, the dynamic response was low. Current demand in optimizing the strength-to-weight ratio of a structure has exposed the structures and machine to vibration problem due to the change in the dynamic properties. The poor design might lead the resonance to lie within the vicinity of the operating frequency of the structure. This may lead to a large undesired vibration which may cause catastrophic damage to the structures and machines, and in the worst case, it may jeopardise human safety.

Dynamic vibration absorber (DVA) is one of the vibration control methods in reducing vibration problems [1–3]. The DVA was first introduced by Frahm [4], which is also called tuned vibration absorber (TVA). It consists of a single-degree-of-freedom (SDOF) oscillating system which can be placed on any structures or machines. This DVA works best in cancelling the vibrations of the primary structure by tuning its natural frequency to coincide with the troublesome frequency of the structure. However, the vibration suppression from the traditional DVA is only effective in a narrow frequency range. In the case of mistuning, it might amplify the vibrations and cause more damage.

Researches on the traditional DVA have expanded since then, and this can be classed into several categories. The first is passive tuned DVA which requires manual tuning to adjust the natural frequency of the DVA to match the modal frequency of the primary structure [5–7]. To obtain the desired natural frequency, very often the stiffness is changed instead of the mass. Although this class of DVA has a tunable mechanism to alter its natural frequency, it may not be suitable in

Technical Editor: Pedro Manuel Calas Lopes Pacheco, D.Sc.

✉ Roszaidi Ramlan
roszaidi@utem.edu.my

[1] Centre for Advanced Research on Energy, Faculty of Mechanical Engineering, Universiti Teknikal Malaysia Melaka, Hang Tuah Jaya, Durian Tunggal, 76100 Melaka, Malaysia

Published online: 08 June 2020

applications with varying frequency. Constant re-tuning of the natural frequency of the structure leads to the invention of the actively tuned vibration absorber [8–10]. However, the main drawback of the active tuned DVA is the efficiency of the control algorithm and power requirement during the tuning process. Semi-active tuned DVA also emerged, with a slightly different purpose. The primary purpose of semi-active tuned DVA is to adjust the amount of active damping or the level of amplitude rather than the natural frequency of the absorber [11, 12].

The advancement in smart materials technology has progressed the passive and active tuned DVA further. Smart materials are capable of changing its stiffness when stimulated. Among many smart materials technology, the use of piezoelectric materials [13–15], shape-memory alloys [16–18] and magnetorheological materials [19–22] are common in the passive and active tuned DVAs. Recently, the mechanism of traditional passive tuned DVA has evolved significantly with the inclusion of the hardening stiffness nonlinearity into the system to widen the vibration suppression bandwidth of the primary structure. The inclusion of nonlinear stiffness reduces the needs of other tuning mechanisms since it is already included and may not be needed due to its wider suppression bandwidth. Although the mechanism is mainly aimed for energy harvesting and vibration isolation research, its purpose and operating principle are the same. They can be easily adapted in the application of nonlinear dynamic vibration absorber (NDVA) [23–27].

The wide frequency response of the DVA can also be generated in a more controlled way by using the piecewise-linear stiffness by using a stopper to limit the motion of the oscillating mass [28–30]. The presence of the stopper hardens the stiffness of the system, thus producing almost similar to the one with the hardening stiffness, which benefits the DVA characteristics, especially in the vibration suppression bandwidth [31]. However, the static and dynamic properties of the NDVA with piecewise-linear stiffness have only been studied in terms of the vertical gap between the beam and the stopper. This paper extends the study by introducing a mechanism which has the capability to vary the vertical gap and the horizontal position of the stopper. In the first part, the static and dynamic properties of the NDVA are experimentally characterized. In the second part, the performance of the NDVA is compared with the linear DVA in terms of vibration suppression bandwidth and the sensitivity towards mistune.

2 Characteristics of restoring force-beam deflection

The schematic of the mechanism to generate piecewise-linear stiffness is shown in Fig. 1. The mechanism is made of a fixed-free cantilever beam of length, L with a concentrated force, f applied at the free end. In order to harden the stiffness, two limit blocks are added to constrain the deflection of the beam. The limit blocks are positioned at a distance away from the fixed end, x_i and from the equilibrium position of the cantilever beam, y_i. The x_i and y_i are referred to in this manuscript as the horizontal position and the vertical gap, respectively, from this point onward. The force–deflection characteristic of the system is derived as a function of x_i and y_i by using the double integration method [32]. Equations (1) and (2) show the force–deflection expression for the constrained cantilever beam when subjected to a force, f

$$f(x_c) = \frac{3EIx_c}{L^3}, \quad x_c < x_o \rightarrow \text{unconstrained} \tag{1}$$

$$f(x_c) = \frac{6EI(3Ly_i - 2x_i x_c - x_i y_i)}{x_i(x_i^3 + 6Lx_i^2 - 9L^2x_i + 2L^3)}, \quad x_c > x_o \rightarrow \text{constrained} \tag{2}$$

where E is the modulus of elasticity, I is the second moment of area and L is the length of the beam. The force–deflection expression of the system comprises of two equations.

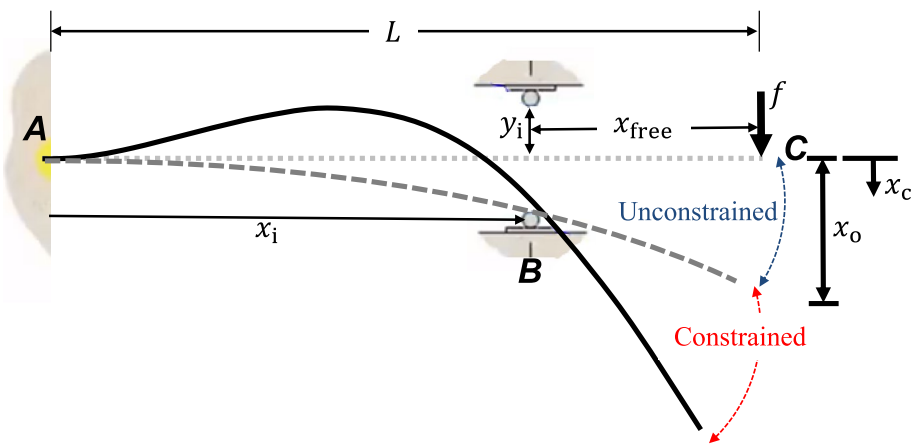

Fig. 1 Schematic of NDVA hardening mechanism constrained by two limit blocks

The first is termed as the unconstrained region while the second is termed as the constrained region. In the unconstrained region, the deflection of the beam is small such that $x_c < x_o$ and this deflection is not affected by the horizontal position, x_i and the vertical gap, y_i. On the other hand, in the constrained region where $x_c > x_o$, the force–deflection expression is affected by both the horizontal position, x_i and the vertical gap, y_i. In this region, the applied force is large enough to cause the deflection of the beam to be constrained by the limit blocks at B. Figure 2 shows the general force–deflection characteristics of the system shown in Fig. 1.

3 Frequency response curve

When a seismic mass m is attached to the free end of the beam in Fig. 1 and the system is based excited, the equation of motion of the system is given by

$$m\ddot{z} + c\dot{z} + k_e z = -m\ddot{x}_b \tag{3}$$

where c is the damping coefficient, $z = x_c - x_b$ is the relative displacement between the tip mass, $x_c = X_c \sin(\omega_b t + \varphi)$ and the harmonic input, $x_b = X_b \sin(\omega_b t)$, k_e is the equivalent stiffness that can be obtained by using the equivalent stiffness method which is also known as the linearization method [33], ω_b is the excitation frequency, and φ is the phase angle between the response and the excitation. Assuming that the response is dominated by the fundamental harmonic, Eq. (3) can be solved using the harmonic balance method to yield the frequency response function plotted in Fig. 3. It is worth to note here that this paper focuses on the experimental study of the subject matter. For analytical and numerical results, readers are suggested to refer to the study described in [28, 31].

The characteristic of the frequency response is almost similar to one with the hardening stiffness reported in [23, 25]. When the excitation frequency is swept up, the response starts to operate in the unconstrained region with a small amplitude under the influence of the restoring force given in Eq. (1). When the excitation frequency is within the vicinity of the equivalent linear natural frequency of the system, the response starts to increase. At this point, the system may respond in two different ways. When the vertical gap y_i is large such that $x_c < x_o$, the response behaves as a linear system following the dotted curve, i.e. 1–2–3–4–6–7 path. Second, when the response is large such that $x_c > x_o$, the system operates under the influence of the restoring force given in Eq. (2). In this case, the response follows the solid curve, i.e. 1–2–4–5 path. In this paper, this broad frequency response is referred to as the high-amplitude branch. Further increase in the excitation frequency causes the response to suddenly drop, i.e. jump-down point at 6. Further increase in excitation frequency causes the response to continue to maintain at low amplitude at high frequencies i.e. point 7. The dashed curve represents the unstable solution for the constrained region's response.

On the other hand, when the excitation frequency is swept from high to low, the response follows the low-amplitude branch under the influence of the restoring force given in Eq. (1) until it reaches point 8. Here, when the motion is not constrained, it behaves linearly again as in the sweep-up frequency excitation before. However, when the motion is constrained, the response follows the solid curve through point 8–4–2 due to the restoring force in Eq. (2) and continues

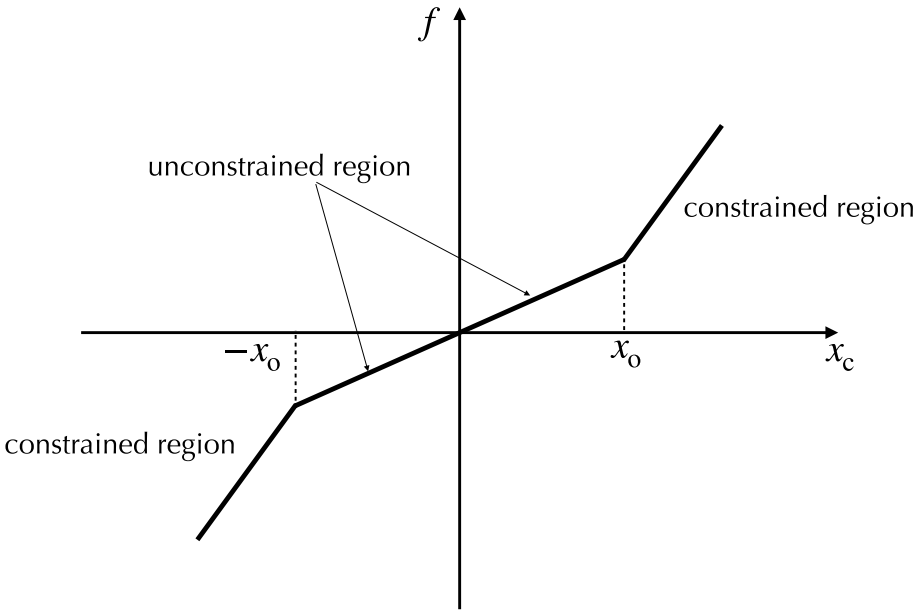

Fig. 2 Restoring force of the cantilever beam against the tip deflection

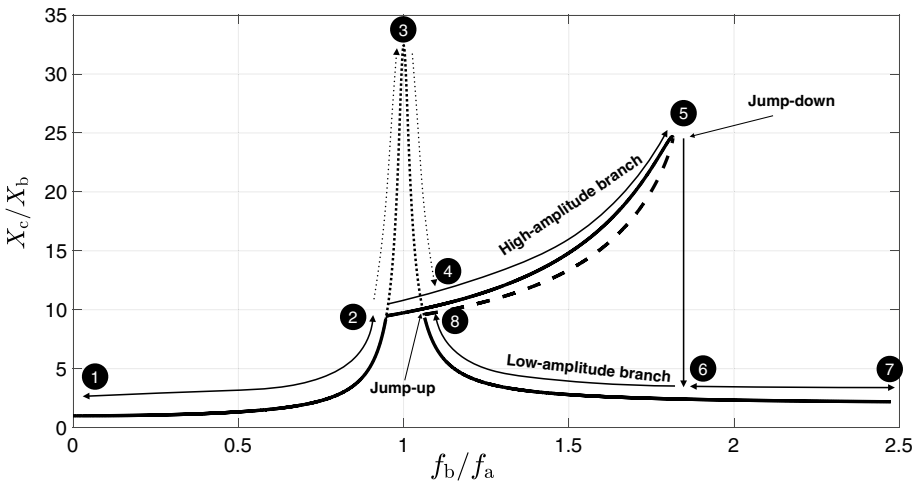

Fig. 3 Frequency response function (FRF) of the based excited single-degree-of-freedom (SDOF) system with a piecewise-linear stiffness against the ratio of the excitation frequency, f_b to the linear natural frequency of the absorber, f_a

further to the starting point under the action of the restoring force in Eq. (1). The amount of damping in the unconstrained region also differs from the one in the constrained region [28].

The high-amplitude branch of the response during the frequency sweep-up is beneficial for vibration absorption purposes due to its ability to produce a wider frequency range. On the other hand, the low-amplitude branch of the response is less favourable as the response only gains in amplitude for a narrow frequency range compared to the high-amplitude branch, similar to the linear system.

4 Mechanism development

The exploded view drawing and the actual photograph of the NDVA employing piecewise-linear stiffness mechanism are shown in Fig. 4a, b, respectively. The mechanism consists of a fixed-free cantilevered beam with a tip mass attached to its free end. The dimension and the mechanical properties of the beam and the mass are given in Table 1. The piecewise-linear stiffness is realized by constraining the motion of the cantilever beam with adjustable limit blocks on both sides of the beam. These blocks are designed such that their vertical gap, y_i and horizontal position, x_i are adjustable. The vertical gap y_i between the block and the equilibrium position of the beam is altered by using the rack and pinion gear mechanism. The rack and pinion system ensures an identical gap for both sides of the beam. The maximum vertical gap between the limit block and the beam that can be achieved is 5 mm. As for the horizontal position, the limit blocks can be moved horizontally to provide different constrained locations from the fixed end of the beam. For this mechanism, the range of the horizontal position that can be adjusted from the fixed end of the beam is from 25 up to 50 mm. Different combinations of the vertical gap and horizontal position result in different force–deflection characteristics of the system, which may affect the dynamic behaviour of the NDVA. The mechanism acts as a linear dynamic vibration absorber with the absence of the limit blocks or when the vertical gap is large.

5 Experimental investigation

The experimental investigation of the NDVA was divided into two parts. The first was to characterize the static and dynamic properties of the proposed NDVA. While the second part of the experiment was to investigate the performance of the proposed NDVA in suppressing the vibration of the primary structure.

5.1 Quasi-static measurement

The quasi-static measurement was implemented to analyse the relationship between the restoring force, f and the tip deflection, x_c. This was done by exciting the base of the NDVA at a frequency of 0.5 Hz. The restoring force of the beam was measured by using Tedea-Huntleigh 1042 load cell, while the tip deflection of the beam was measured by using the Keyence IL-065 laser triangular sensor. The setup for the quasi-static measuring equipment is illustrated schematically in Fig. 5.

5.2 Dynamic measurement (characterization of the NDVA)

The dynamic measurement was conducted to investigate the dynamic behaviour of the proposed NDVA for each of the horizontal position and vertical gap configurations conducted in the quasi-static measurement. The setup for the dynamic measurement is illustrated schematically in Fig. 6.

During the measurement, the NDVA was firmly placed on the ETS L215M electrodynamic shaker so that the system

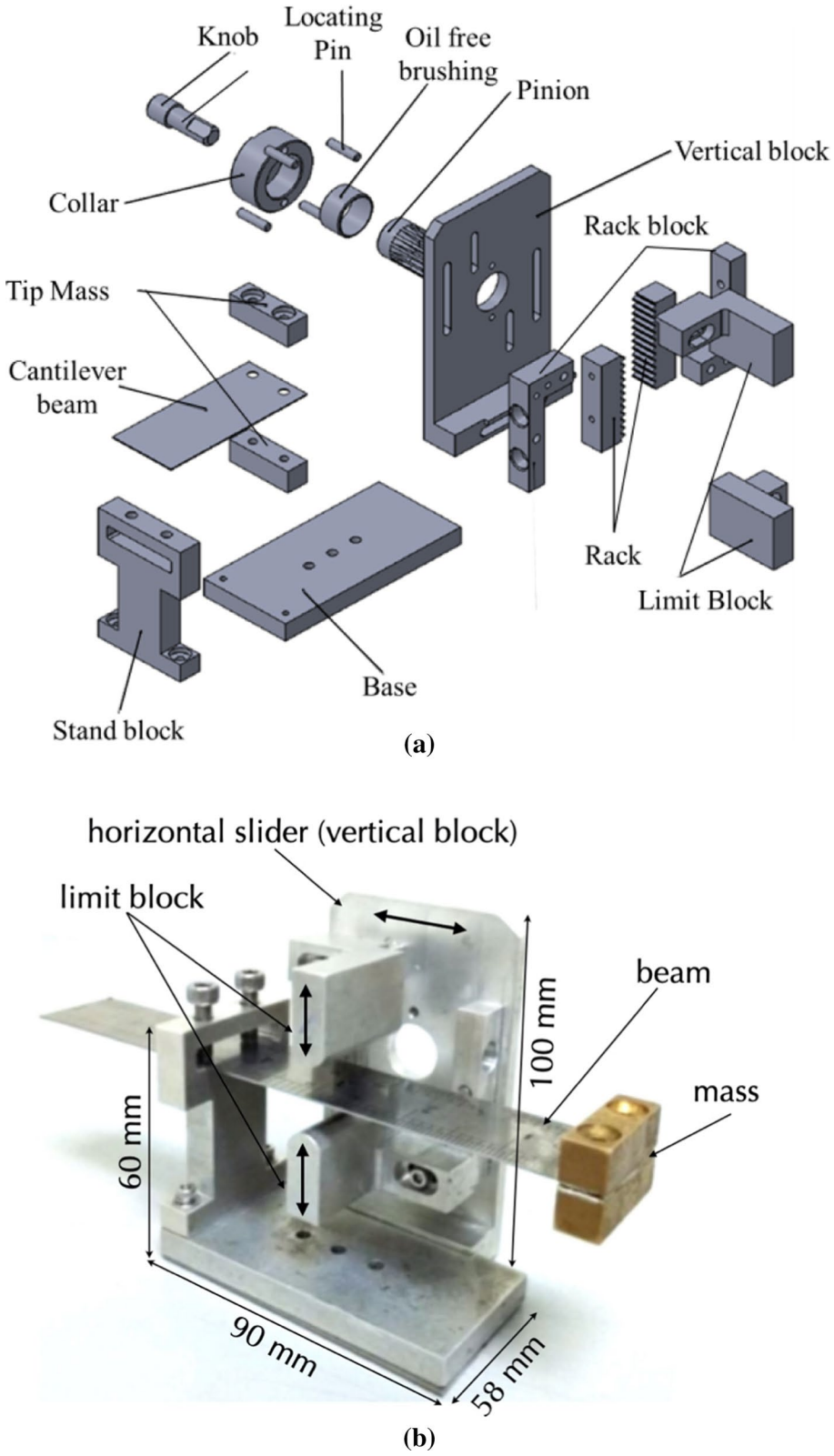

Fig. 4 **a** The exploded view drawing of the mechanism and **b** actual photograph of the mechanism

was base excited. The excitation signal from the shaker was generated using the Vibration Research Medallion II shaker controller, which is connected to the shaker through ETS MPA100 power amplifier. The device was then excited harmonically with increasing frequency (sweep-up) from 10 to 40 Hz at a rate of 0.5 Hz/s and then at decreasing

Table 1 Mechanical properties and dimension of the steel beam and the brass tip mass

Part	Parameter	Value
Cantilever beam	Young's modulus, E	1.60×10^{11} N/m^2
	Thickness of beam, t	0.75 mm
	Length, L	120 mm
	Breadth, b	26 mm
Tip mass	Mass, m	40 g

frequency (sweep-down) from 40 to 10 Hz with the same sweep rate. The amplitude of the input displacement X_b was kept constant throughout the measurement by using the feedback signal from the accelerometer mounted on the shaker. The acceleration of the tip mass and the feedback acceleration signal were measured by using Dytran 3225F1 accelerometers. The results obtained were analysed in the form of absolute transmissibility, X_c/X_b and the phase difference between the amplitude of the displacement response of

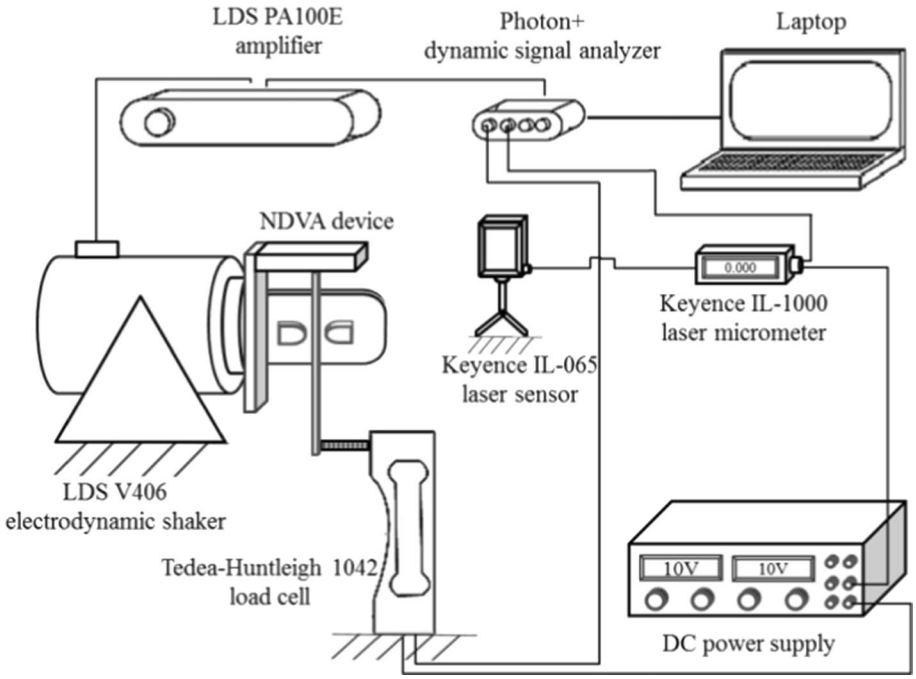

Fig. 5 Schematic of the quasi-static measurement setup

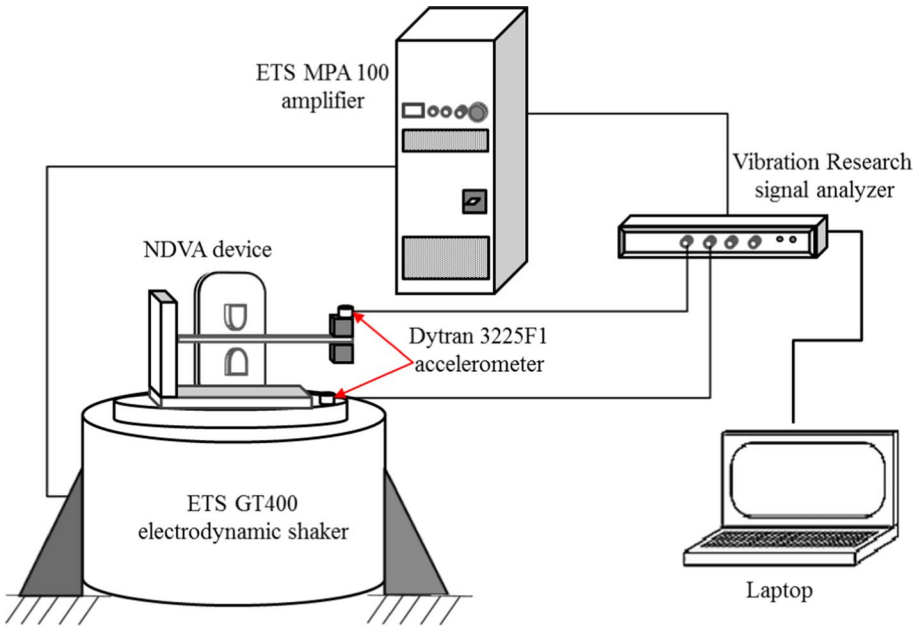

Fig. 6 Schematic of the dynamic measurement setup

NDVA seismic mass, X_c and the amplitude of displacement input provided by the shaker, X_b.

5.3 Dynamic measurement (performance of the NDVA)

The performance of the NDVA to widen the vibration suppression bandwidth and its tolerance towards mistuning compared to the linear DVA were also investigated in the dynamic measurement. The mechanical properties and dimension of the beam used as the primary structure are given in Table 2, and the setup to measure the performance of the NDVA is illustrated schematically in Fig. 7.

In the measurement, the linear DVA or NDVA was attached at the tip of the free end of the primary beam structure where the amplitude at the first modal frequency was the highest. A Dytran 1051V1 force sensor was attached between the TIRA S51140 electrodynamic shaker and the beam structure to measure the dynamic force applied to the primary structure during excitation. Three Dytran 3225F1 accelerometers were also attached at three different measuring points, namely at the shaker base, primary structure and at the DVA mass to measure the input and the responses.

The effect of mistuning on the performance of both linear DVA and NDVA was investigated by inspecting the vibration reduction amplitude at the first natural frequency of the primary structure and the separation of the two newly formed resonance frequencies. To quantify the degree of mistuning, each of the absorber was tuned at different frequency ratios, f_a/f_s i.e. $f_a/f_s = 0.75$, $f_a/f_s = 0.85$ and $f_a/f_s = 1.0$ where f_a is the linear natural frequency of the DVA and f_s is the first natural frequency of the primary structure, i.e. 19.5 Hz given in Table 2. The linear natural frequency of the DVA was changed by changing the effective length of the beam. The targeted value of the vibration reduction is when $X_s \leq X_{st}$ where X_s is the amplitude response of the primary structure at the first natural frequency and X_{st} is the static deflection of the primary structure [34]. The range of the excitation frequency applied to the primary structure was similar to the one used in characterizing the dynamic property of the NDVA in the previous section. However, only one input displacement was used and the amplitude of the input displacement of the electrodynamic shaker X_b was kept constant at 0.5 mm during the sweep-up or sweep-down of the excitation frequency.

Table 2 Mechanical properties and dimension of the primary beam structure

Specification	Value
Modulus of elasticity, E_s	2.1×10^{11} N/m^2
Density, ρ_s	1.02×10^{4} kg/m^3
Length, L_s	0.70 m
Breath, b_s	0.050 m
Thickness, d_s	0.015 m
Beam mass, M	5.39 kg
First natural frequency, f_s	19.5 Hz

Subscript 's' refers to the "primary structure"

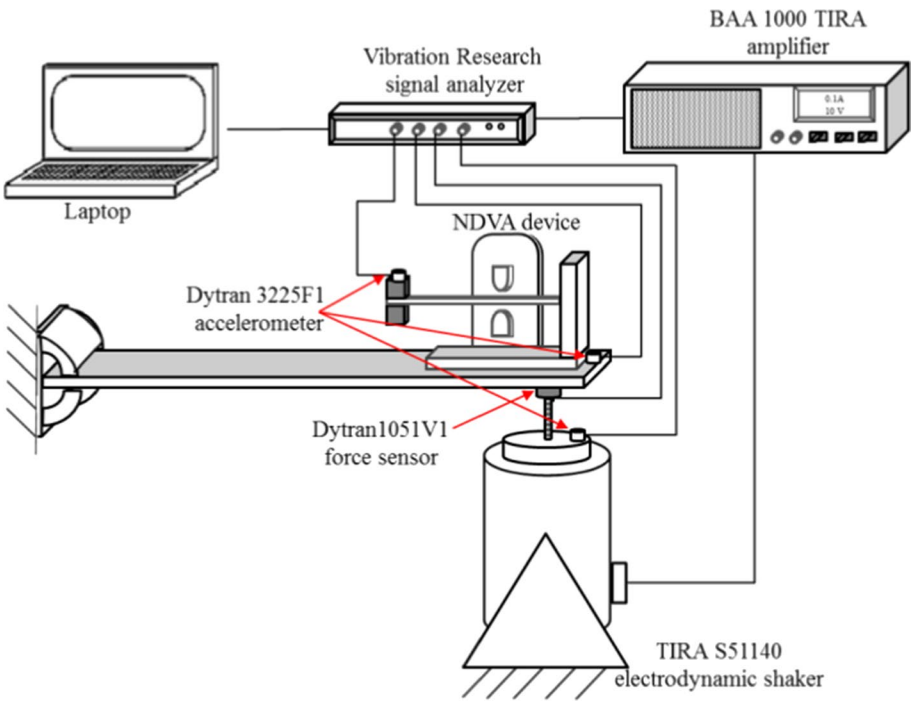

Fig. 7 Schematic of the dynamic performance measurement setup

6 Results and discussion

6.1 Force–deflection characteristic

Figure 8a, b shows the measured force–deflection characteristics for different x_i and y_i configurations, respectively. The result for different horizontal positions x_i shows that when $x_i = 25$ mm, there is insufficient tip deflection of the beam to cause it to reach the constrained region, i.e. $x_c < x_o$, thus the beam follows the straight line of the unconstrained region. Under this configuration, the restoring force is linearly proportional to the tip deflection and the system is composed of a single linear stiffness given in Eq. (1). As x_i increases, the force–deflection of the beam shows piecewise-linear restoring force characteristic with two different stiffness regions which are termed as the low-stiffness region (unconstrained region) and high-stiffness region (constrained region) as illustrated earlier in Fig. 2.

It can also be observed in Fig. 8b that the gradient of the force–deflection curves in the constrained region for different vertical gaps y_i is almost constant for all configurations. On the other hand, the gradient of the force–deflection curves differs for different horizontal positions, x_i. In particular, the gradient increases as x_i increases. This shows that the gradient of the force–deflection in the constrained region is dependent upon the free end length of the beam, measured from the location of the limit block, x_{free} as annotated in Fig. 1 and is not dependent upon the vertical gap, y_i. Overall,

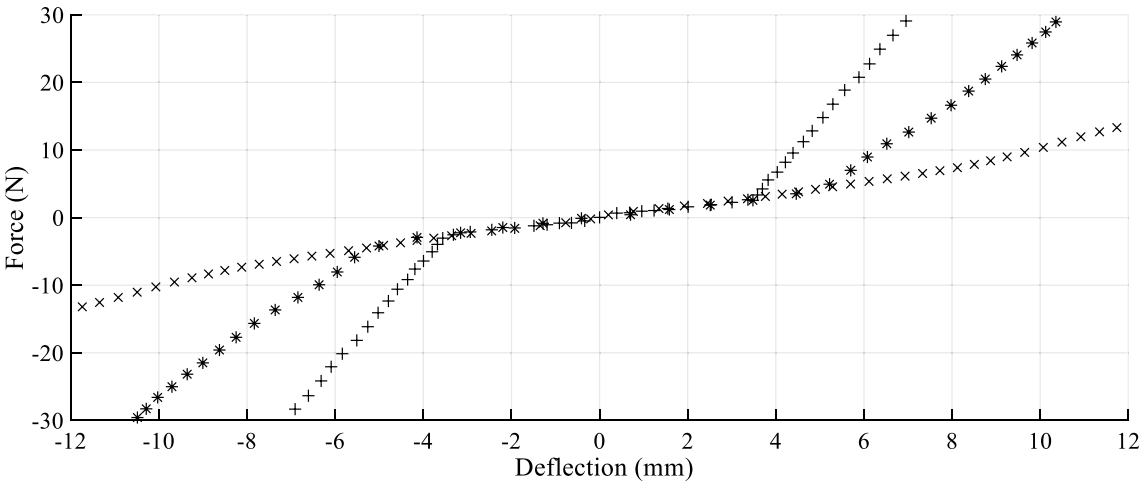

(a)

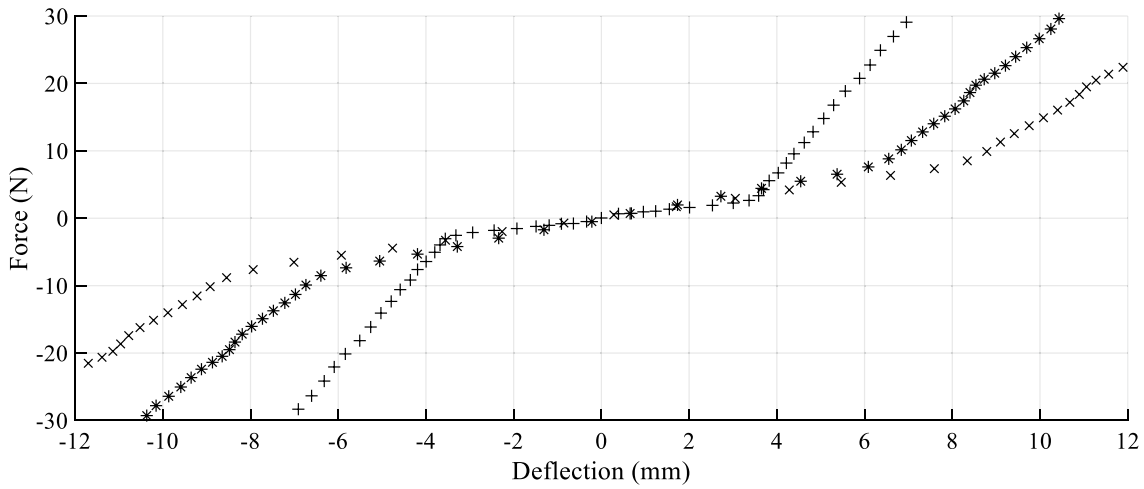

(b)

Fig. 8 The measured force–deflection curves for **a** different horizontal positions, x_i while the vertical gap y_i is fixed at 1 mm: $x_i = 25$ mm (×), $x_i = 35$ mm (*), and $x_i = 45$ mm (+) and **b** different vertical gaps, y_i while horizontal position x_i is fixed at 45 mm; $y_i = 1$ mm (+), $y_i = 2$ mm (*), and $y_i = 3$ mm (×)

an increase in y_i expands the unconstrained region while an increase in x_i expands the constrained region.

6.2 *Dynamic behaviour of the NDVA: effect of limit block position (horizontal position x_i and vertical gap y_i)*

The effect of horizontal position x_i on the dynamic response of the NDVA under harmonic excitation is presented in Fig. 9 while the effect of the vertical gap y_i is plotted in Fig. 10. From both figures, it can be seen that the jump-down point is significantly affected by the change in the horizontal position and the vertical gap while the jump-up point is less affected. The jump-down frequency increases as x_i increases and y_i decreases. For all configurations, the phase difference at the maximum response, i.e. jump-down point, along the sweep-up frequency response is 90°.

As elaborated in the previous section, the dynamic response of the NDVA is highly dependent on the free end length of the beam, x_{free}, i.e. the distance from the free end of the beam to the limit block, and the contact point (vertical gap) controls the required tip deflection for the constrained motion. The shorter the free end length x_{free} and the closer the contact point of the beam to the limit blocks, the larger the frequency bandwidth due to the expanded constrained region. This explains the reason why the amplitude of the

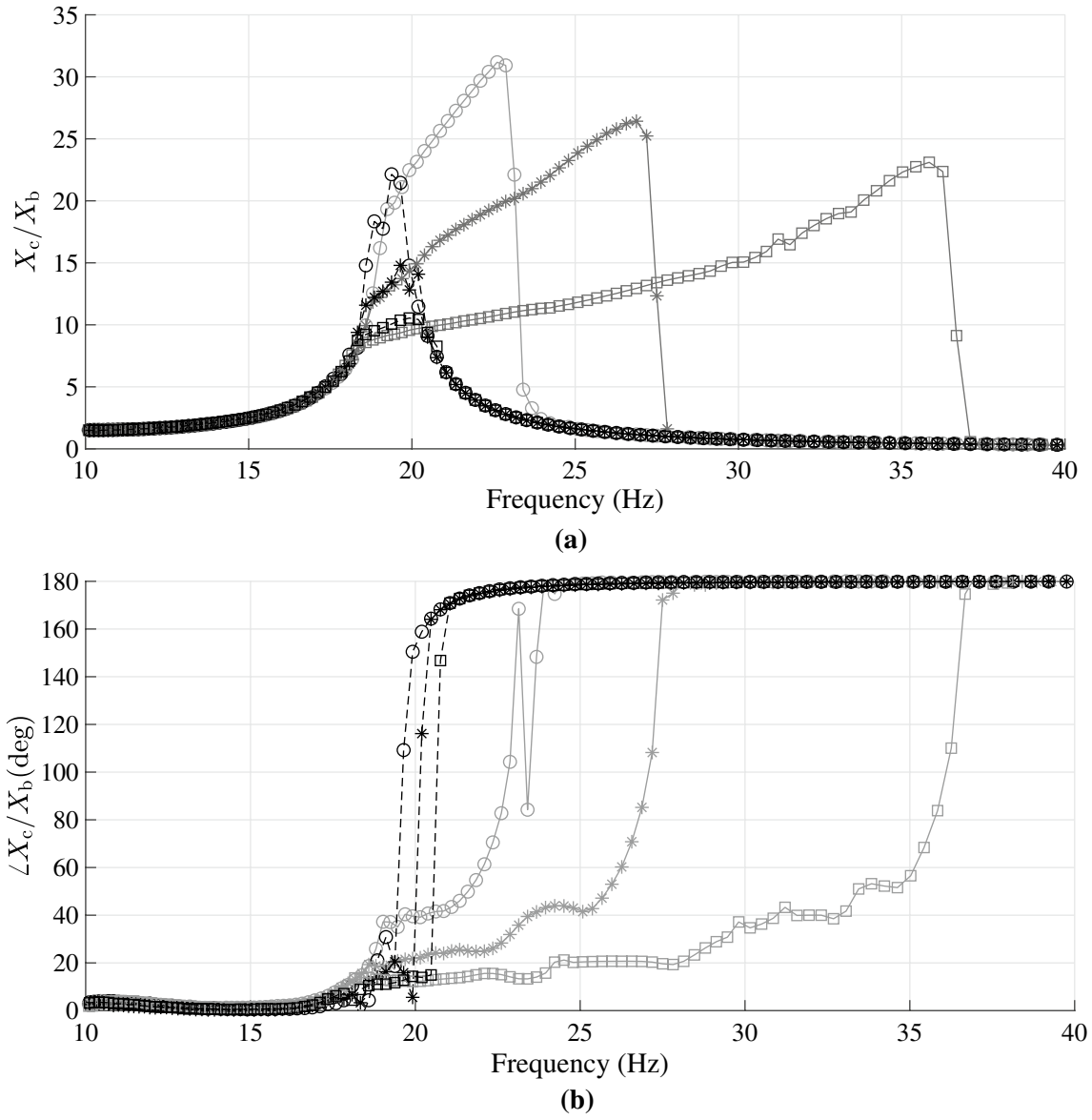

Fig. 9 **a** Absolute transmissibility and **b** phase angle for different horizontal positions, x_i, i.e. 25 mm (o), 35 mm (*) and 45 mm (□) [sweep-up (—), sweep-down (--) with $y_i = 1$ mm and $X_b = 1$ mm

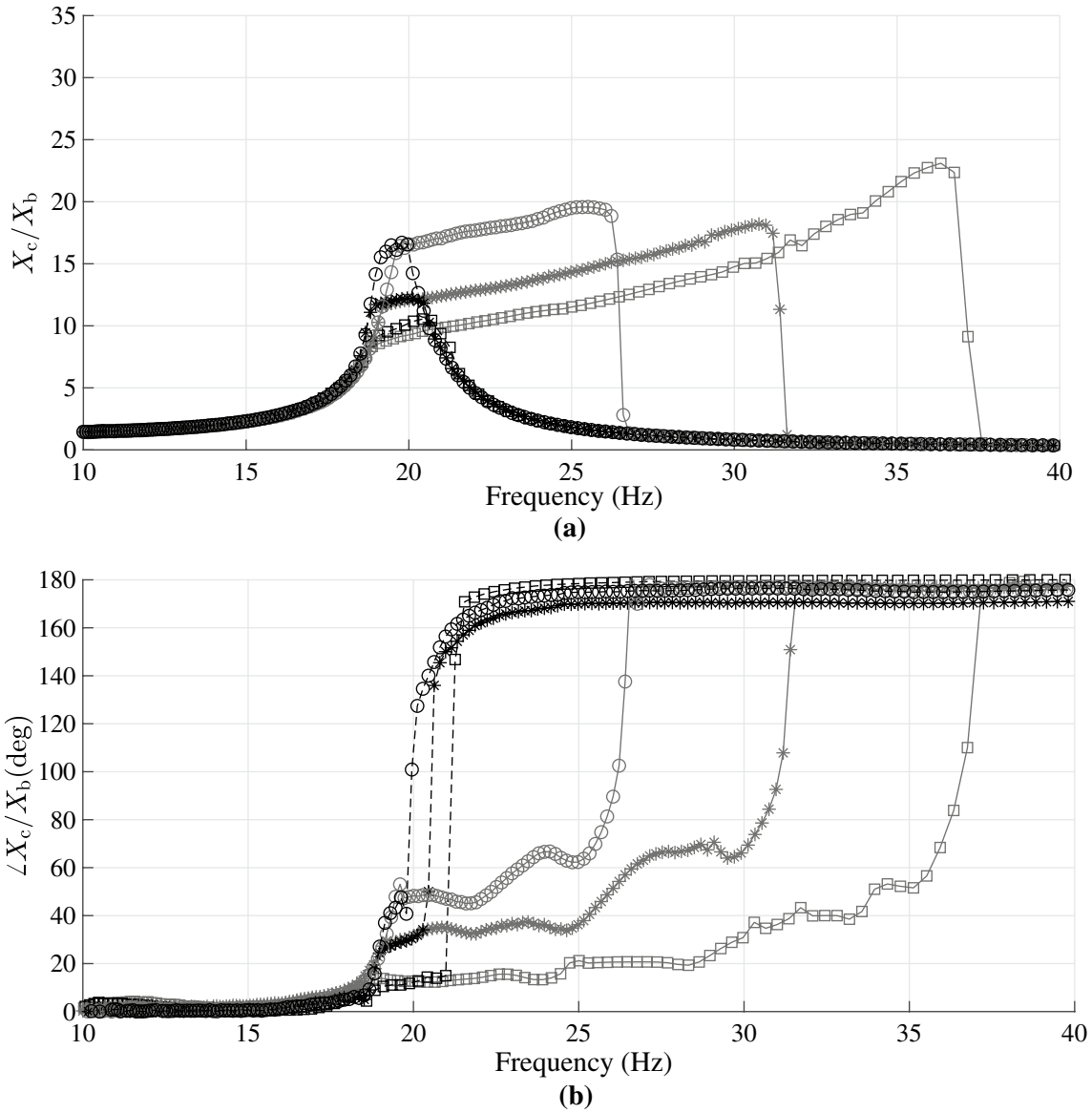

Fig. 10 **a** Absolute transmissibility and **b** phase angle for different vertical gaps, y_i, i.e. 3 mm (o), 2 mm (*) and 1 mm (□) [sweep-up (—), sweep-down (--)] with $x_i = 45$ mm and $X_b = 1$ mm

response with the largest x_i and the smallest y_i are the smallest among the three configurations but with the highest jump-down frequency.

Another interesting point to note on the effect of the horizontal position, x_i and the vertical gap, y_i is the rate of change of amplitude of the response with respect to the excitation frequency. The rate of change of amplitude with respect to the excitation frequency decreases with x_i but is independent upon y_i. The expected difference in the gradient of frequency response curves from different x_i and y_i configurations of the high-amplitude branch is due to the amount of constrained region's stiffness which is dependent upon the free end length, x_{free}. For different y_i configurations, the amount of the tip deflection to reach the limit block differs from one configuration to the other. However, the contact points are all similar for all configurations giving rise to the same free end length, x_{free}, thus producing the same gradient of the high-amplitude branch. As for the different x_i configurations, an increase in x_i shortens the free end length, x_{free}. This increases the constrained region's stiffness and lowers the rate of change of the amplitude with respect to the excitation frequency, as the response progresses further to the right on the high-amplitude branch towards the jump-down point.

The amount of damping may also influence the response of the NDVA. For this mechanism, the damping was estimated experimentally. The damping factor in the

unconstrained region is termed as ζ_1 and ζ_2 for the constrained region. The amount of the unconstrained region's damping ζ_1 is determined to be 0.01 and is similar for all configurations in Figs. 9 and 10 since all of them have a similar natural frequency. The constrained region's damping ζ_2 for different horizontal positions in Fig. 9, i.e. 25 mm, 35 mm and 45 mm are 0.019, 0.029 and 0.038, respectively. Unfortunately, the constrained region's damping for different vertical gaps in Fig. 10 is not available due to the lack of experimental data. However, based on Fig. 9, the amount of damping is expected to increase as the gap gets smaller due to the impact and frictional losses.

The availability of the two tuning parameters, x_i and y_i, provides beneficial tuning capability which cannot be found in the existing nonlinear hardening mechanism, especially the ones that use magnetic stiffness to create the nonlinear effect as reported in [23, 25]. In these reported mechanisms, the degree of nonlinearity is partly contributed by the ratio between the nonlinear stiffness and the equivalent linear stiffness. These two stiffnesses depend on the gap between the magnets and commonly, the degree of the nonlinearity increases with the decrease in the gap.

However, the jump-down and the jump-up points in the dynamic response of the reported mechanisms depend on both the equivalent linear stiffness (similar to the unconstrained region's stiffness in the proposed NDVA) and the nonlinear stiffness (i.e. constrained region's stiffness). Depending on the magnetic pole configuration, decreasing the gap may increase or decrease the equivalent natural frequency. The change in the linear natural frequency shifts the jump-down and jump-up points accordingly. The transition of the jump-down and the jump-up points makes it difficult to effectively targeting the troublesome frequency to be suppressed.

Unlike all the drawbacks of the existing magnetic nonlinear hardening mechanisms, the jump-up of the proposed NDVA mechanism does not change very much with the change in the horizontal distance x_i and the vertical distance y_i. The "fixed" jump-up point makes it easier to target the troublesome frequency.

6.3 Performance of the linear DVA

The receptance function of the primary structure and the absolute transmissibility between the linear DVA and the primary structure for each tuning frequency ratio, f_a/f_s together with their phase angle when the linear DVA is attached to the primary structure, are shown in Fig. 11.

Based on Fig. 11, the vibration suppression of the primary structure at its first natural frequency is optimized when the linear natural frequency of the absorber is tuned to match the first natural frequency of the primary structure, i.e. $f_a/f_s = 1.0$. It is also noted that the smallest vibration suppression amplitude occurs at the targeted disturbing frequency, i.e. $f_b/f_s = 1$. It can also be seen that the phase difference between the primary structure and linear DVA at this frequency is 90° which indicates maximum equivalent damping or maximum power flow provided by the DVA [35]. The two newly formed resonance frequencies of the primary structure as a result of linear DVA attachment are evenly located on either side of the original modal frequency.

The performance of the linear DVA in suppressing the vibration at the targeted disturbing frequency when its natural frequency is not tuned to match the first natural frequency, i.e. $f_a/f_s = 0.75$ and $f_a/f_s = 0.85$ deteriorates significantly. The vibration level at $f_a/f_s = 1$ for each tuned frequency ratio is larger than the targeted vibration level. This is because the phase difference for the two mistuned cases is not 90° at the targeted frequency, which indicates the inability of the DVA to generate the maximum amount of damping to suppress the vibration. Nevertheless, the mistuned absorbers perform very well at $f_b/f_s = 0.75$ and $f_b/f_s = 0.85$, which is away from the targeted frequency. The level of damping in the system may contribute to the good performance of the system. This can be either in terms of the level of suppression or the width of the suppression bandwidth. However, here the damping in the system may have an insignificant contribution to the performance since it is measured for three different configurations, operating at three different frequencies.

Figure 11 also shows that there is no valid vibration reduction frequency bandwidth for the mistuned DVAs as the vibration amplitude of the primary structure at the targeted frequency $f_b/f_s = 1$ is larger than the targeted value. This shows that the linear DVA has a low tolerance towards mistune, with even a slight mistune causes its performance to deteriorate. What more important is that a slight mistune brings the response of the primary structure closer to one of the new resonance peaks. This resulting response of the primary structure in the vicinity of the newly formed resonance peaks may amplify the vibration even larger than the original response. In the case when the linear DVA is over-tuned with respect to the primary structure, the vibration suppressed point will shift to the right, in contrast to the under tuned before, i.e. $f_a/f_s < 1$.

6.4 Performance of the NDVA

The measurement of the effect of NDVA on the structural vibration was done slightly different from the linear DVA. Here, the excitation frequency was swept up and down throughout the measurement due to the hysteresis. Figures 12, 13 and 14 show the receptance function of the primary structure, the transmissibility between the DVA, X_c and the primary structure, X_s, the phase angle between the DVA and the primary structure under different tuned frequency

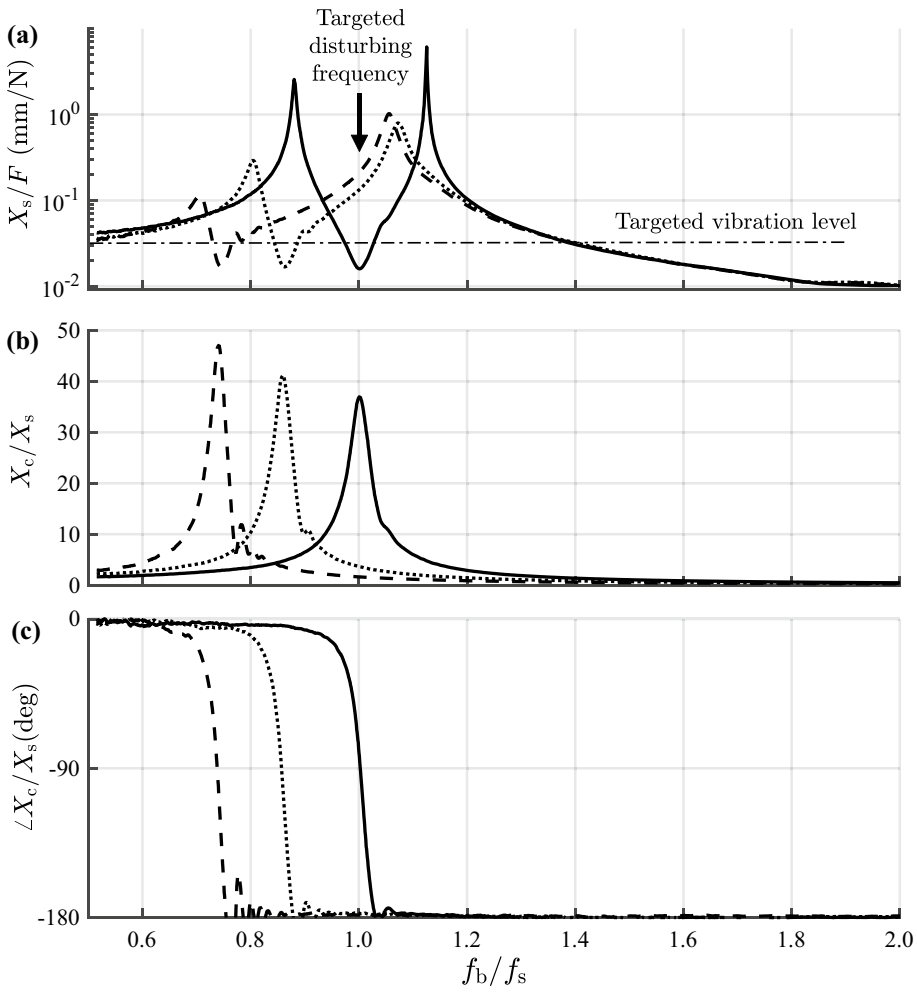

Fig. 11 Measured **a** frequency response of the primary structure, **b** transmissibility between the DVA, X_c and the primary structure, X_s and **c** phase angle between the DVA and the primary structure for $f_a/f_s = 1.0$ (—), $f_a/f_s = 0.85$ (⋯) and $f_a/f_s = 0.75$ (--) at $X_b = 0.5$ mm. Damping ratio, $\zeta_1 = 0.014$ ($f_a/f_s = 1.0$), $\zeta_1 = 0.012$ ($f_a/f_s = 0.85$) and $\zeta_1 = 0.010$ ($f_a/f_s = 0.75$)

ratios, f_a/f_s. The receptance of the linear DVA discussed in the previous section is overlaid with its respective tuned frequency ratio NDVA to compare the performance. In general, the presence of the NDVA seems to broaden the separation between the first resonance peak and the second resonance peak during the sweep-up of the excitation frequency. During the sweep-down excitation, the response is almost similar to the linear DVA.

Referring to Fig. 12, the level of vibration at the targeted frequency is slightly larger than the targeted level. This is because, for the DVA to apply maximum damping to the primary structure, DVA must lag the primary structure by 90°. This is not the case for the NDVA since the 90° phase lag occurs at a higher frequency, i.e. at the jump-down point, which brings down the vibration level of the primary structure at high frequencies. This may not be entirely beneficial for excitation close to resonance frequency since the suppression of the vibration of the primary structure is not required at high frequency in the first place because the undesired large vibration is only concentrated around the resonance region. Nevertheless, the NDVA has increased the second natural frequency of the structure to a much higher frequency compared to the linear DVA. In this case, when the excitation frequency is operating at the first natural frequency of the primary structure, the linear DVA is the better choice. However, when the excitation frequency operates at high frequency, then the NDVA is preferred.

The significant improvement in the NDVA over the linear DVA starts to be seen in Fig. 13 when $f_a/f_s = 0.85$ where its suppressed vibration level outperforms its linear counterpart at the targeted frequency. The lower linear natural frequency of the DVA also brings down the jump-down frequency. The decrease in the jump-down frequency decreases the separation of the two new resonance peaks. This, in effect, reduces the vibration suppression bandwidth. In this case, the vibration suppression bandwidth spreads wider above the targeted frequency in proportion to the high-amplitude branch response of the NDVA shown in Fig. 13b.

The level of force generated by the NDVA, which is viewed as the level of displacement response, also increases with the smaller tuned frequency ratio, as shown in Fig. 14 for the case where $f_a/f_s = 0.75$. Although the smaller tuned frequency ratio results in a much-reduced response at around the resonant frequency of the structure, care needs to be

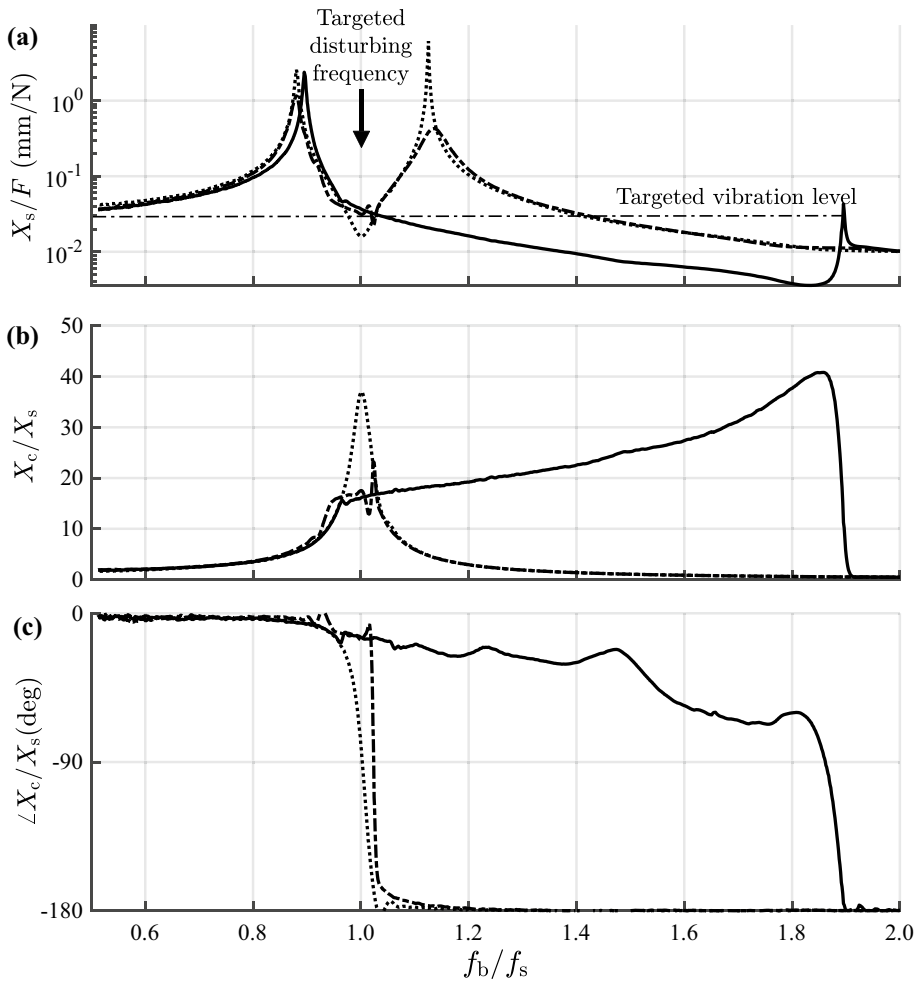

Fig. 12 Measured **a** frequency response of the primary structure, **b** transmissibility between the DVA, X_c and the primary structure, X_s and **c** phase angle between the DVA and the primary structure for $f_a/f_s = 1.0$ [NDVA sweep-up (—), NDVA sweep-down (--), linear DVA (···)] when $X_b = 0.5$ mm

taken since the second resonance during the forward frequency sweep appears around the structure's original natural frequency. As the tuned frequency ratio decreases, the response exhibits non-smooth dynamics which is consistent to results reported in [29, 31]. The non-smooth response could be due to the beat vibration caused by the engagement of the beam and the limit block. Chaotic vibration resulting from the nonlinear characteristic of the system may also cause the non-smooth response [31].

Table 3 summarizes the comparison of the performance of the linear DVA and the NDVA. Based on Table 3, the superiority of the absorber is achieved by considering its effect during the sweep-up response, which means that the response is on the high-amplitude branch in the multi-stable solutions frequency range. If the NDVA is on the down-sweep response, the performance of the NDVA is at par with the linear DVA because the response is not operating on the high-amplitude branch as discussed in the previous section.

Thus for the vibration suppression to be effective, it is mandatory to keep the NDVA to vibrate on its high-amplitude branch to avoid amplitude amplification of the primary structure which is caused by the resonance peak produced by the backward frequency sweep. However, as long as the frequency range of interest is far away from the jump-down point, the tendency of the response to operating on the high-amplitude branch is high due to the readily available initial conditions [24]. As the frequency of interest gets closer to the jump-down point, the system may not easily start with the right initial conditions to operate on the high-amplitude branch. In practice, the actual jump-down point occurs, maybe, at a slightly lower frequency.

Based on this study, the performance of the NDVA is generally better compared to the linear DVA. The significant improvement in the performance can be achieved by only restricting the motion of the existing linear DVA using a limit block on both sides of the beam. The tuning capability of the NDVA is more robust in terms of vibration reduction bandwidth and the level of vibration suppression. However, the NDVA is only effective when the linear natural frequency of the NDVA is tuned to be less than the primary structure's natural frequency, $f_a/f_s \leq 1$. This is to ensure that the targeted disturbing frequency lies within the broad high-amplitude branch response of the NDVA and the suppression range covers both sides of the targeted frequency. Optimum

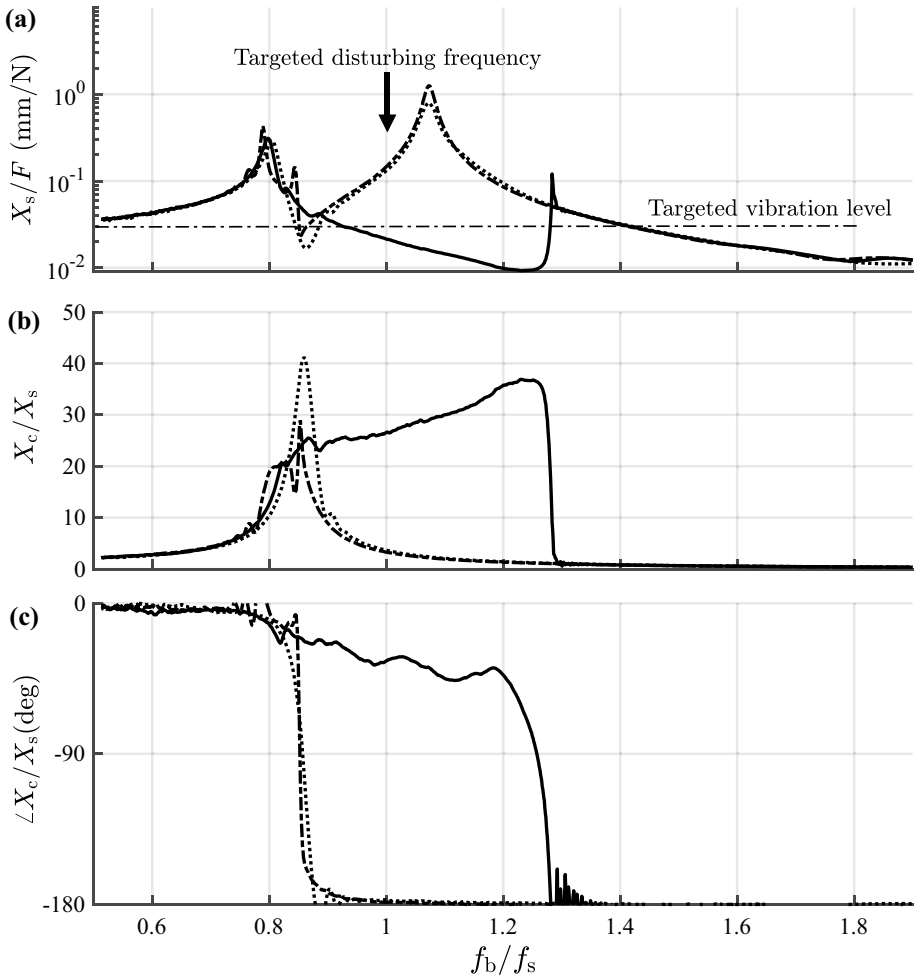

Fig. 13 Measured **a** frequency response of the primary structure, **b** transmissibility between the DVA, X_c and the primary structure, X_s and **c** phase angle between the DVA and the primary structure for $f_a/f_s = 0.85$ [NDVA sweep-up (—), NDVA sweep-down (--), linear DVA (···)] when $X_b = 0.5$ mm

tuning is yet to be totally explored for this NDVA. However, based on the results presented in Figs. 9 and 10, the level of the vibration suppression and the bandwidth of the NDVA may be changed by carefully altering the horizontal position, x_i and the vertical gap, y_i.

7 Conclusion

The newly designed NDVA with the use of a piecewise-linear stiffness mechanism performs better than the linear DVA, especially in terms of vibration suppression bandwidth and shows that it can cope with mistuning better. This is made possible by the constrained region's stiffness which hardens the stiffness. The hardened stiffness skews the maximum response of the NDVA to a high frequency at a much slower rate with respect to the excitation frequency. This enlarges the half-power bandwidth of the NDVA, thus increasing the vibration suppression bandwidth. The good thing is that this NDVA can be realized by putting two limit blocks on the existing linear DVA to constrain the motion of the beam. However, the better performance of the NDVA over the linear DVA is only possible when the NDVA operates on the high-amplitude branch. Otherwise, the performance is similar to the linear DVA.

In general, the piecewise-linear stiffness mechanism provides a better tuning ability than the nonlinear hardening stiffness mechanism, especially the ones with nonlinear magnetic stiffness. In the nonlinear magnetic hardening stiffness, tuning is slightly difficult due to the shift of the linear natural frequency and the jump points as the nonlinearity increases or decreases. Unlike the nonlinear hardening system employing magnetic stiffness, the proposed piecewise-linear stiffness mechanism has a fixed natural frequency. At the same time, the bandwidth and the level of vibration suppression can be altered by adjusting the horizontal position and the vertical gap of the limit blocks.

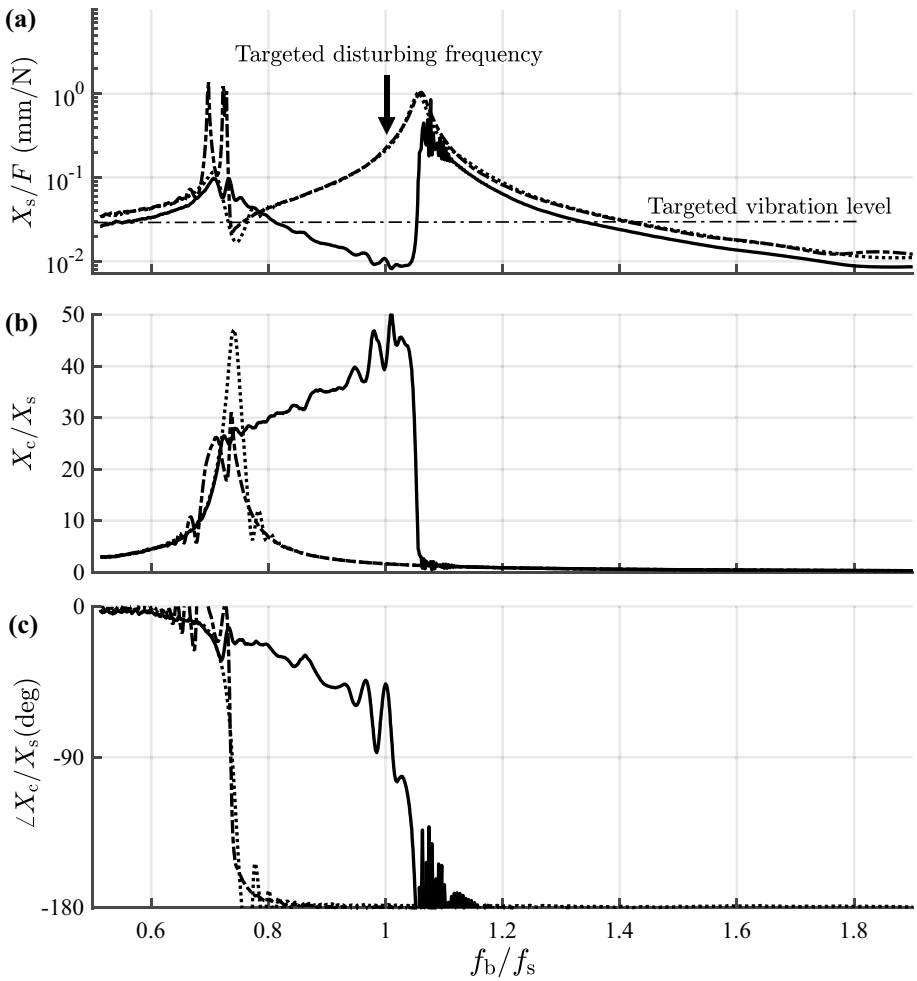

Fig. 14 Measured **a** frequency response of the primary structure, **b** transmissibility between the DVA, X_c and the primary structure, X_s and **c** phase angle between the DVA and the primary structure for $f_a/f_s = 0.75$ [NDVA sweep-up (—), NDVA sweep-down (--), linear DVA (···)] when $X_b = 0.5$ mm

Table 3 Comparison of the response of the primary structure under the action of linear DVA and NDVA for different tuned frequency ratios

Type of DVA	Frequency ratio, f_a/f_s	Ratio of the vibration response of the primary structure over the targeted vibration level at $f_b/f_s = 1$	First resonance (Hz)	Second resonance (Hz)	Vibration reduction bandwidth (Hz)
Linear DVA	1	0.53	17.1	21.8	1.2
	0.85	4.33	15.7	20.8	0
	0.75	8.0	13.7	20.4	0
NDVA (up-sweep)	1.0	1.16	17.5	36.9	17.7
	0.85	0.7	15.6	25.0	7.6
	0.75	0.4	13.9	20.8	4.8
NDVA (down-sweep)	1	1.03	17.5	22.2	1.4
	0.85	4.83	15.6	20.8	0
	0.75	7.33	13.9	20.8	0

Acknowledgements The authors would like to acknowledge the financial support from the Ministry of Higher Education Malaysia and the Universiti Teknikal Malaysia Melaka through the Fundamental Research Grant Scheme (FRGS/1/2016/TK03/FKM-CARe/F00318).

References

1. Love JS, Haskett TC, Morava B (2018) Effectiveness of dynamic vibration absorbers implemented in tall buildings. Eng Struct 176:776–784

2. Pais T, Boote D (2017) Developments of tuned mass damper for yacht structures. Ocean Eng 141:249–264
3. Gafsi W, Chaari R, Masmoudi N, Khabou MT, Chaari F, Haddar M (2017) Modeling of a passive absorber in milling tool machine. Appl Acoust 128:94–110
4. Frahm H (1911) Device for Damping Vibrations of Bodies. United States of America 989958:1–9
5. Wright RI, Kidner MRF (2004) Vibration absorbers: a review of applications in interior noise control of propeller aircraft. J Vib Control 10(8):1221–1237
6. Brennan MJ (2006) Some recent developments in adaptive tuned vibration absorbers/neutralisers. Shock Vib 13:531–543
7. Kela L, Vähäoja P (2009) Recent studies of adaptive tuned vibration absorbers/neutralizers. Appl Mech Rev 62:1–9
8. Gao JX, Cheng L (2004) Modelling of a high performance piezoelectric actuator assembly for active and passive vibration control. Smart Mater Struct 13:384–392
9. Chen Y, Fuh C, Tung P (2005) Application of voice coil motors in active dynamic vibration absorbers. IEEE Trans Magn 41(3):1149–1154
10. Kai C, Huang A (2014) Active vibration absorber design for mechanical systems with frequency-varying excitations. J Vib Control 20(15):2338–2351
11. Setareh M (2001) Application of semi-active tuned mass dampers to base-excited systems. Earthq Eng Struct Dyn 30(3):449–462
12. Zihao L, Wanyou L, Yali Y (2016) A study of a beam-like electromagnetic vibration absorber. J Vib Control 22(11):2559–2568
13. Davis CL (2000) An actively tuned solid-state vibration absorber using shunting of piezoelectric stiffness. J Sound Vib 232(3):601–617
14. Bonello P, Brennan MJ, Elliott SJ (2005) Vibration control using an adaptive tuned vibration absorber with a variable curvature stiffness element. Smart Mater Struct 14(5):1055–1065
15. Herold S, Mayer D (2016) Adaptive piezoelectric absorber for active vibration control. Actuators 5(7):1–13
16. Saadat S, Salichs J, Noori M, Hou Z, Davoodi H, Bar-On I, Suzuki Y, Masuda A (2002) An overview of vibration and seismic applications of NiTi shape memory alloy. Smart Mater Struct 11:218–229
17. Rustighi E, Brennan MJ, Mace BR (2004) A shape memory alloy adaptive tuned vibration absorber: design and implementation. Smart Mater Struct 14(1):19–28
18. dos Santos FA, Nunes J (2018) Toward an adaptive vibration absorber using shape-memory alloys, for civil engineering applications. J Intell Mater Syst Struct 29(5):729–740
19. Deng H, Gong X, Wang L (2006) Development of an adaptive tuned vibration absorber with magnetorheological elastomer. Smart Mater Struct 15(5):N111–N116
20. Deng HX, Gong XL (2007) Adaptive tuned vibration absorber based on magnetorheological elastomer. J Intell Mater Syst Struct 18(12):1205–1210
21. Hirunyapruk C, Brennan MJ, Mace BR, Li WH (2010) A tunable magneto-rheological fluid-filled beam-like vibration absorber. Smart Mater Struct 19(5):055020
22. Kumbhar SB, Chavan SP, Gawade SS (2018) Adaptive tuned vibration absorber based on magnetorheological elastomer-shape memory alloy composite. Mech Syst Signal Process 100:208–223
23. Mann BP, Sims ND (2009) Energy harvesting from the nonlinear oscillations of magnetic levitation. J Sound Vib 319(1–2):515–530
24. Ramlan R, Brennan MJ, Mace BR, Kovacic I (2010) Potential benefits of a non-linear stiffness in an energy harvesting device. Nonlinear Dyn 59(4):545–558
25. Ramlan R, Brennan MJ, Mace BR, Burrow SG (2012) On the performance of a dual-mode non-linear vibration energy harvesting device. J Intell Mater Syst Struct 23(13):1423–1432
26. Ledezma-Ramirez DF, Ferguson NS, Brennan MJ, Tang B (2015) An experimental nonlinear low dynamic stiffness device for shock isolation. J Sound Vib 347:1–13
27. Gatti G, Brennan MJ, Tang B (2019) Some diverse examples of exploiting the beneficial effects of geometric stiffness nonlinearity. Mech Syst Signal Process 125:4–20
28. Soliman MSM, Abdel-Rahman EM, El-Saadany EF, Mansour RR (2008) A wideband vibration-based energy harvester. J Micromech Microeng 18(11):115021
29. Hoffmann D, Folkmer B, Manoli Y (2009) Fabrication, characterization and modelling of electrostatic micro-generators. J Micromech Microeng 19(9):094001
30. Yao H, Cao Y, Zhang S, Wen B (2018) A novel energy sink with piecewise linear stiffness. Nonlinear Dyn 94:2265–2275
31. Shui X, Wang S (2018) Investigation on a mechanical vibration absorber with tunable piecewise-linear stiffness. Mech Syst Signal Process 100:330–343
32. Hibbeler RC (2016) Mechanics of materials, 10th edn. Pearson, London
33. Wagg D, Neild S (2010) Nonlinear vibration with control for flexible and adaptive structure. Solid mechanics and its applications, vol 170. Springer, London
34. Hsu Y (2013) The performance of a nonlinear dynamic vibration absorber. PhD Thesis, University of Southampton
35. Soong TT, Dargush GF (1997) Passive energy dissipation systems in structural engineering, 1st edn. Wiley, England